Supplemental Methods.

Osteogenic differentiation: Mineralization: In vitro osteogenic differentiation was performed as previously described [S1-2]. Unless otherwise stated, reagents were sourced from Sigma Aldrich. Briefly, confluent monolayers were incubated for 21 days in CCM containing 10^{-8} M dexamethasone, 50 µg mL^{-1} ascorbic acid and 5 mM β-glycerol phosphate for 21 days with changes every 2 days. The monolayers were then fixed with formalin, washed in distilled water, and then stained with 40 mM Alizarin Red S (ARS) pH 4.0 to visualize calcified matrix. After a brief wash in distilled water, micrographs were taken using an inverted microscope (Nikon Eclipse, TE200) fitted with a Nikon DXM1200F digital camera. Quantification of differentiation was performed based on a previously described protocol [S1]. Briefly, ARS was recovered from the stained monolayers by 15 min incubation in 10% (v/v) acetic acid warmed to 50°C. The recovered ARS was then quantified by absorbance spectroscopy at 420 nm using a commercial microplate reader (Fluostar Omega, BMG Labtech, Cary NC).

Alkaline phosphatase: Assays of alkaline phosphatase (ALP) activity were performed as described previously [S3-4] using a colorimetric assay. Briefly, monolayers (in 4 cm^2 12-well Corning plates) were washed in PBS, then in ALP reaction buffer (50 mM Tris-HCl pH 9.0 containing 100 mM KCl and 1 mM $MgCl_2$). One half-mL ALP reaction buffer was added to each well followed by 0.5 mL of p-nitrophenol phosphate (PNPP) (Thermo Scientific, Rockford, IL). The conversion of PNPP to nitrophenolate was plotted by monitoring absorbance at 405 nm every 30 s using a commercial plate reader. After 10 min, the monolayers were washed with PBS and subjected to cell enumeration by a fluorescent DNA labeling assay based on Sytox dye incorporation [S4]. Briefly, monolayers were lysed by freezing, followed by the addition of PBS containing 0.1% (v/v) Triton X-100 and 2 units per mL of *Eco*RI and 2 units per mL of *Hind*III to release DNA from the dense monolayers. Plates were incubated in a humidified chamber at 37°C

with rocking for 12-15 h then centrifuged at 1500 g for 15 min. Samples of solubilised, clarified lysate were diluted if necessary and mixed with 0.001 volumes of Sytox green dye (Life Technologies, Grand Island, NY). Cell number was ascertained by comparing fluorescence at 488ex/504em with known standards using a commercial plate reader.

Osteoprotegerin assay: ELISA assays were performed as previously described [S4] on conditioned media using a commercially available kit (OPG Duo-kit, R&D systems, Minneapolis, MN).

Adipogenic differentiation: In vitro adipogenic differentiation was performed as previously described [S2]. Briefly, confluent monolayers were incubated for 21 days in CCM supplemented with 0.5 µM dexamethasone, $5x10^{-8}$ M isobutylmethylxanthine, and $5x10^{-7}$ M indomethacin (Sigma-Aldrich). Media were changed every 2 days. After 21 days, the adipogenic cultures were fixed in 10% (v/v) formalin and lipid deposits were stained with fresh 0.5% (w/v) oil red-O solution (Sigma) in 60 % (v/v) isopropanol in phosphate buffered saline (PBS) for 20 min. The monolayers were rinsed with PBS and visualized using an inverted microscope (Nikon Eclipse, TE200) fitted with a Nikon DXM1200F digital camera.

Chondrogenic differentiation: In vitro chondrocyte differentiation was performed as previously described [S5-6] on 250,000 pelleted cells. Briefly, cell pellets were incubated in high glucose Dulbecco's MEM containing 10^{-7}M dexamethasone, 50 µg mL^{-1} ascorbate-2-phosphate, 40 µg mL^{-1} proline, 100 µg mL^{-1} pyruvate and ITS plus premix (Sigma-Aldrich) with media changes every 2-3 days. After 21 days, the pellets were washed in PBS and fixed in 4% (v/v)

paraformaldehyde, embedded in paraffin, sectioned, and then stained with toluidine blue to visualize proteoglycans and chondrocyte lacunae.

Immunophenotyping: MSCs were recovered by trypsinization and incubated with fluorophore-tagged antibodies or isotype controls (Becton Dickinson Pharmingen, Franklin Lakes, NJ or Beckman Coulter, Indianapolis, IN) for 30 min in PBS containing 2 % (v/v) FBS. After washing, at least 20,000 events were analyzed on a Cytomics FC500 flow cytometer (Beckman Coulter) and data were processed using the manufacturers' software (CXP, Beckman Coulter). The following clones were used: CD11b (clone BEAR1), CD14 (RMO52), CD19 (J3-119), CD29 (MAR4), CD34 (581), CD36 (FA6.152), CD44 (G44-26), CD45 (J.33), CD49a (SR84), CD49b (Gi9), CD49c (C3 II.1), CD49e (IIA1), CD51 (23C6), CD73 (AD2), CD79a (HM47), CD90 (Thy-1/310), CD105 (IG2), CD146 (TEA1/34), CD166 (3A6), HLA-A,B,C (G46-2.6), and HLA-DP,DQ,DR (Tu39).

Carboxyfluorescein-succinimidyl-ester proliferation assay: Discarded in-line filter sets were acquired from Scott and White Hospital Blood Center and peripheral blood mononuclear lymphocytes (PBLs) were isolated. Proliferation assays were performed as described previously [(S7)]. Human allogenic PBMCs were labeled with 2.5 µM carboxyfluorescein diacetate, succinimidyl ester (CFSE; Molecular Probes/Invitrogen) according to the manufacturer's instructions. For each assay, 50,000 PBLs were co-cultured with 5,000 OEhMSCs in triplicates in RPMI 1640 medium (Gibco) supplemented with 10% human AB serum (Corning cellgro), 100 units · mL-1 penicillin G, and 100 µg · mL-1 streptomycin for up to 7 days. As a positive control, lymphocyte expansion was stimulated by CD3/CD28 complexed Dynabeads (Gibco). Cultures

were analyzed on a Cytomics FC500 flow cytometer (Beckman Coulter) and data were processed using the manufacturers' software (CXP, Beckman Coulter).

Quantitative RT-PCR (qRT-PCR) and microarray assays: The number of OEhMSCs present on Gelfoam or BGF cultures was measured using qRT-PCR for glyceraldehyde-3-phosphate dehydrogenase (GAPDH). For this purpose, 0.25 cm^3 constructs were subjected to total RNA extraction using a commercially available kit (High Pure kit, Roche, Indianapolis, IN). One tenth of the total RNA generated was then used to synthesize cDNA (Superscript III kit, Invitrogen) and one tenth of the resultant cDNA was transferred to a single qRT-PCR reaction. A commercial PCR master mix (Evagreen, Biotium, Hayward, CA) was used with GAPDH-specific primers (**Table S1**) [S8]. Cells were enumerated by comparison with known OEhMSC standards. One-half μg cDNA was used for each reaction and relative BMP2 expression levels were calculated using the $2^{-\Delta\Delta CT}$ method [S9]. The level of GAPDH transcription was employed to normalize measurements. For microarray assays, unless otherwise stated, all reagents were purchased from Affymetrix. A total of 2.0 μg RNA was used for assays. Briefly, double-stranded cDNA was synthesized using the One-Cycle cDNA Synthesis Kit and cleaned with the Sample Cleanup Module. Biotin-labeled cRNA was synthesized using the GeneChip IVT Labeling Kit and quantified spectrophotometrically (SmartSpec, Bio-Rad). Twenty-μg of biotin-labeled cRNA was hybridized to HG-U133 Plus 2.0 arrays with hybridization controls. After 16-h hybridization, the arrays were washed and stained in the Fluidics Station 450 using the GeneChip Hybridization Wash and Stain Kit. The arrays were then scanned using the GeneChip Scanner G7 and Command Console software. Transcripts of interest generated from the array data were confirmed using RT-PCR.

Immunoblotting: Immunoblotting was performed using Novex reagents (Invitrogen). Antibodies were mouse anti-β-actin (AC-15, Sigma-Aldrich), rabbit-anti human type VI collagen (Novus Biologicals, Littleton, CO), rabbit-anti human type XII collagen (Novus), goat anti-mouse IgG-peroxidase conjugate (Biomeda, Foster, CA), goat anti-rabbit IgG-peroxidase conjugate (Biomeda).

Supplemental tables:

Table S1: Primers used in this study.

Target	Sequence	Conditions	Reference / notes
human GAPDH	FOR ctctctgctcctcctgttcgac REV tgagcgatgtggctcggct	SYBR-green 60ºC	(S8) RTPrimerDB ID_1242*
human collagen I	FOR gaacgcgtgtcatcccttgt REV gaacgaggtagtctttcagcaaca	SYBR-green 60ºC	RTPrimerDB ID_1089* *marginal cross-reactivity detected in mock samples.
human collagen III	FOR gggaacaacttgatggtgctact REV tcagacatgagagtgtttgtgcaa	SYBR - green 60ºC	RTPrimerDB ID_4463* *marginal cross-reactivity detected in mock samples.
human collagen V	FOR cacaacttgcctgatggaataaca REV gcagggtacagctgcttggt	SYBR - green 60ºC	RTPrimerDB ID_1091*
Human collagen VI	FOR ccatcgtgcgcagcc REV tgcgccgactcgtgc	SYBR - green 60ºC	n/a
human collagen XI	FOR gactatcccctcttcagaactgttaac REV cttctatcaagtggtttcgtggttt	SYBR - green 60ºC	RTPrimerDB ID_1736*
human collagen XII	FOR cttccattgaggcagaagtt REV agacacaagagcagcaatga	SYBR - green 60ºC	(S10)
human collagen XV	FOR cgtgttagagatggctgga REV gtttggtggaggcagaag	SYBR - green 60ºC	(S11)
human collagen XIV	FOR tccgaggaatggtataaccgg REV tggaccaggaacactgacagg	SYBR - green 60ºC	(S12)
human BMP2	FOR cccagcgtgaaaagagagac REV gagaccgcagtccgtctaag	SYBR-green 55ºC	Generated by the Oligo Perfect™ algorithm (Invitrogen)

Table S2: Transcriptional up-regulation of secreted osteogenic ligands by OEhMSCs upon adherence to BGF.

Gene	Accession	Entrez Number	Fold Change (multiple entries refer to alternative probe sets)
BMP2	NM_001200	650	**18.35**
Cartilage oligomeric matrix protein	NM_000095	1311	**13.86**
BMP8B	NM_001720	656	**9.28**
BMP6	AI123471	654	**8.69**
Collagen V α3	AI984221	50509	**7.08, 5.79**
Collagen X α1	AI376003	1300	**5.16, 3.26**
Periostin	AY140646	10631	**5.06, 2.63, 2.13**
Wnt 2B	AB045117	7482	**4.88**
Parathyroid hormone like hormone	J03580	5744	**4.27**
Collagen VI α1	M20776	1291	**4.19**
Latent transforming growth factor beta binding protein 3	BF059064	4054	**3.73**
Collagen III α1	AU146808	1281	**3.77**
BMP1	AF318323	649	**3.62**
Collagen XI α1	NM_001854	1301	**3.21, 2.74**
BMP5	AL133386	653	**2.85**
Alkaline phosphatase	S76738	249	**2.66**
Collagen I α2	AA628535	1278	**2.65**
Collagen I α1	AI743621	1277	**2.35**
BMP 4	D30751	652	**2.06**
Matrix metallopeptidase 13	NM_002427	4322	**2.14**
Fibroblast growth factor 18	AI798863	8817	**2.2**
Osteomodulin	AI765819	4958	**2.02**

Table S3: Transcriptional up-regulation of secreted angiogenic ligands by OEhMSCs upon adherence to BGF.

Gene	Accession	Entrez Number	Fold Change (multiple entries refer to alternative probe sets)
Endothelin 1	NM_001955	1906	**8.51**
Fibroblast growth factor 1	X59065	2246	**5.05, 2.91, 2.15**
Fibroblast growth factor 9	AL583692	2254	**4.75**
Transforming growth factor beta1	NM_000660	7040	**4.41**
Transforming growth factor alpha	M31172	7039	**3.87**
Transforming growth factor beta2	NM_003238	7042	**2.52**
Placental growth factor	AK023843	5228	**2.34**
Thrombospondin 1	AW956580	7057	**2.11**

Supplemental References.

S1. Gregory CA, Gunn WG, Peister A, Prockop DJ. An Alizarin red-based assay of mineralization by adherent cells in culture: comparison with cetylpyridinium chloride extraction. Anal Biochem. 2004 Jun 1;329(1):77-84.

S2. Gregory CA, Prockop DJ. Fundamentals of Culture and Characterization of Mesenchymal Stem/Progenitor Cells (MSCs) from Bone Marrow Stroma. In: Freshney RIS, Stacey GN and Auerbach JM, editors. Culture of Human Stem Cells. Hoboken NJ: Wiley-Liss; 2007. p. 208.

S3. Krause U, Harris S, Green A, et al. Pharmaceutical modulation of canonical Wnt signaling in multipotent stromal cells for improved osteoinductive therapy. Proc Natl Acad Sci U S A. 2010 Mar 2;107(9):4147-52.

S4. Krause U, Seckinger A, Gregory CA. Assays of osteogenic differentiation by cultured human mesenchymal stem cells. Methods Mol Biol. 2011;698:215-30.

S5. Sekiya I, Colter DC, Prockop DJ. BMP-6 enhances chondrogenesis in a subpopulation of human marrow stromal cells. Biochem Biophys Res Commun. 2001 Jun 8;284(2):411-8.

S6. Sekiya I, Vuoristo JT, Larson BL, Prockop DJ. In vitro cartilage formation by human adult stem cells from bone marrow stroma defines the sequence of cellular and molecular events during chondrogenesis. Proc Natl Acad Sci U S A. 2002 Apr 2;99(7):4397-402.

S7. Lyons AB, Parish CR. Determination of lymphocyte division by flow cytometry. J Immunol Methods. 1994 May;171(1):131-7.

S8. Carraro G, Albertin G, Forneris M, Nussdorfer GG. Similar sequence-free amplification of human glyceraldehyde-3-phosphate dehydrogenase for real time RT-PCR applications. Mol Cell Probes. 2005 Jun;19(3):181-6.

S9. Livak KJ, Schmittgen TD. Analysis of relative gene expression data using real-time quantitative PCR and the 2(-Delta Delta C(T)) Method. Methods. 2001 Dec;25(4):402-8.

S10. Nemoto T, Kajiya H, Tsuzuki T, Takahashi Y, Okabe K. Differential induction of collagens by mechanical stress in human periodontal ligament cells. Arch Oral Biol. 2010 Dec;55(12):981-7.

S11. Lisignoli G, Codeluppi K, Todoerti K, et al. Gene array profile identifies collagen type XV as a novel human osteoblast-secreted matrix protein. J Cell Physiol. 2009 Aug;220(2):401-9.

S12. Schmidt A, Lorkowski S, Seidler D, Breithardt G, Buddecke E. TGF-beta1 generates a specific multicomponent extracellular matrix in human coronary SMC. Eur J Clin Invest. 2006 Jul;36(7):473-82.

Supplemental Figure legends.

Fig. S1. Generation of the femoral segmental defect model in mice. Panel A: Photographs of the pin assembly compared to a standard murine femur (above). **Panel B:** pin assembly after installation. **Panel C:** Pin assembly with associated GF collar. **Panel D:** reconstruction of μCT scan of installed pin demonstrating penetration of the trabecular bone. **Panel E-H:** Photographs of procedure and radiography of live mouse harboring pin.

Fig. S2. Characterization of representative hMSC preparation used in this study. Panel A: Flow cytometry of hMSCs demonstrating typical immunoprofile. **Panel B-D:** Mineralized monolayers stained with alizarin red S at low (**panel B**) and high (**panel C**) power compared with a non-stimulated control culture (**panel D**). **Panel E-G:** Adipocyte monolayers stained with oil red O at low (**panel E**) and high (**panel F**) power compared with a non-stimulated control culture (**panel G**). **Panel H-I:** toluidine-blue stained sections of chondrocyte micro-mass cultures demonstrating purple deposits of sulphated proteoglycan around lacunae.

Fig. S3. Representative three dimensional reconstructions of murine femora that received a pin-stabilized segmental defect treated with hMSCs (**panel A**) or OEhMSCs (**panel B**). The images at *left* and *center* indicate the pin in blue and the bone at 80% (*left*) and 20% (*center*) opacity and the images on the *right* present the bone at 100% opacity in the absence of the pin.

Fig. S4. Polar moment of inertia measurements at the proximal and distal ends of femoral defects treated with OEhMSCs and hMSCs in the absence of solid scaffold (values are generated by taking the mean of 3 adjacent axial images). Statistical testing was performed by ANOVA and Tukey post-test. *P*-values key: $P<0.05$ = *, $P<0.01$=**.

Fig. S5. Polar moment of inertia measurements at the proximal and distal ends of femoral defects treated with OEhMSCs and hMSCs in the presence of BGF or GF. (values are generated by taking the mean of 3 adjacent axial images). Statistical testing was performed by ANOVA and Tukey post-test. *P*-values key: $P<0.01$=**, $P<0.005$=***.

Fig. S6. Representative three dimensional reconstructions of murine femora that received a pin-stabilized segmental defect treated with BGF and OEhMSCs. **Panel A and B** are renderings of specimens that had fully bridged the defects whereas **panel C and D** are representative specimens with incomplete bridging. The images at *left* and *center* indicate the pin in blue and the bone at 80% (*left*) and 20% (*center*) opacity and the images on the *right* present the bone at 100% opacity in the absence of the pin.

Fig. S7. Diagrammatic summary of receptor/ligand complexes that are transcriptionally up-regulated by OEhMSCs upon attachment to BGF as compared to GF. Red stars indicate up-regulated genes. Data generated by the DAVID software suite utilizing the KEGG database.

Fig. S8. Diagrammatic summary of signal transduction pathways with components that are transcriptionally up-regulated by OEhMSCs upon attachment to BGF as compared to GF. Red stars indicate up-regulated genes. Data generated by the DAVID software suite utilizing the KEGG database.

Fig. S1

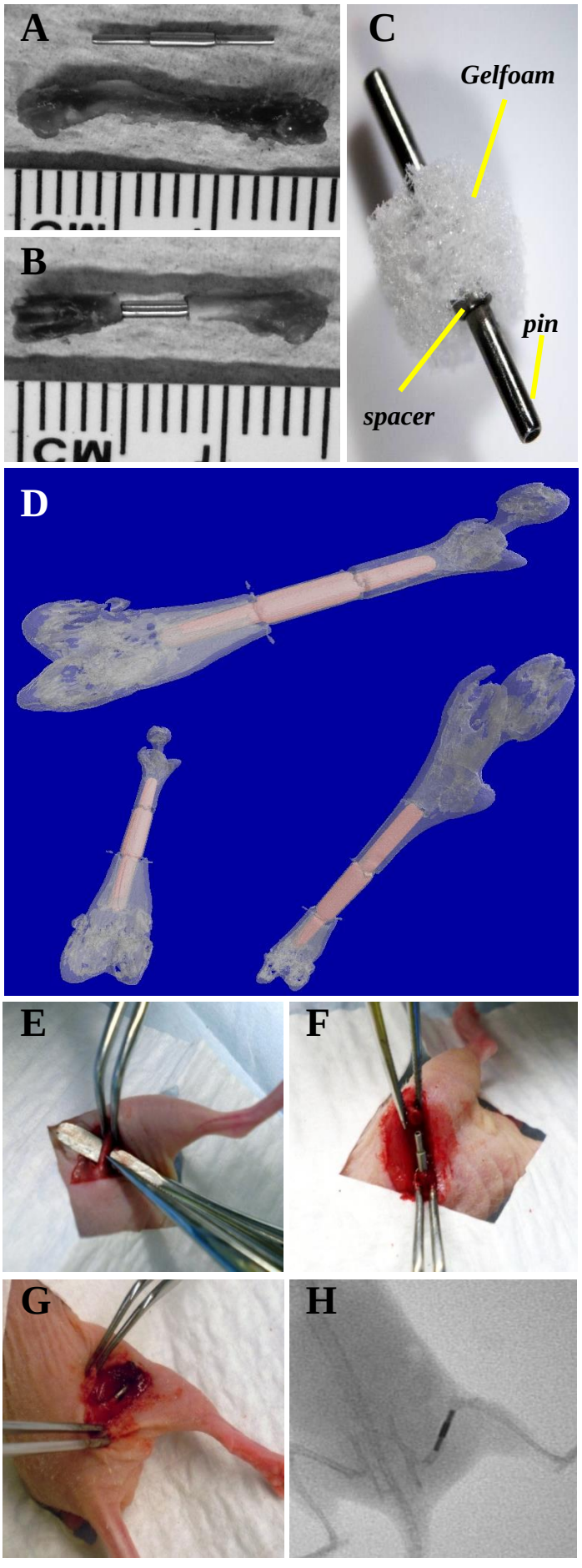

Fig. S2

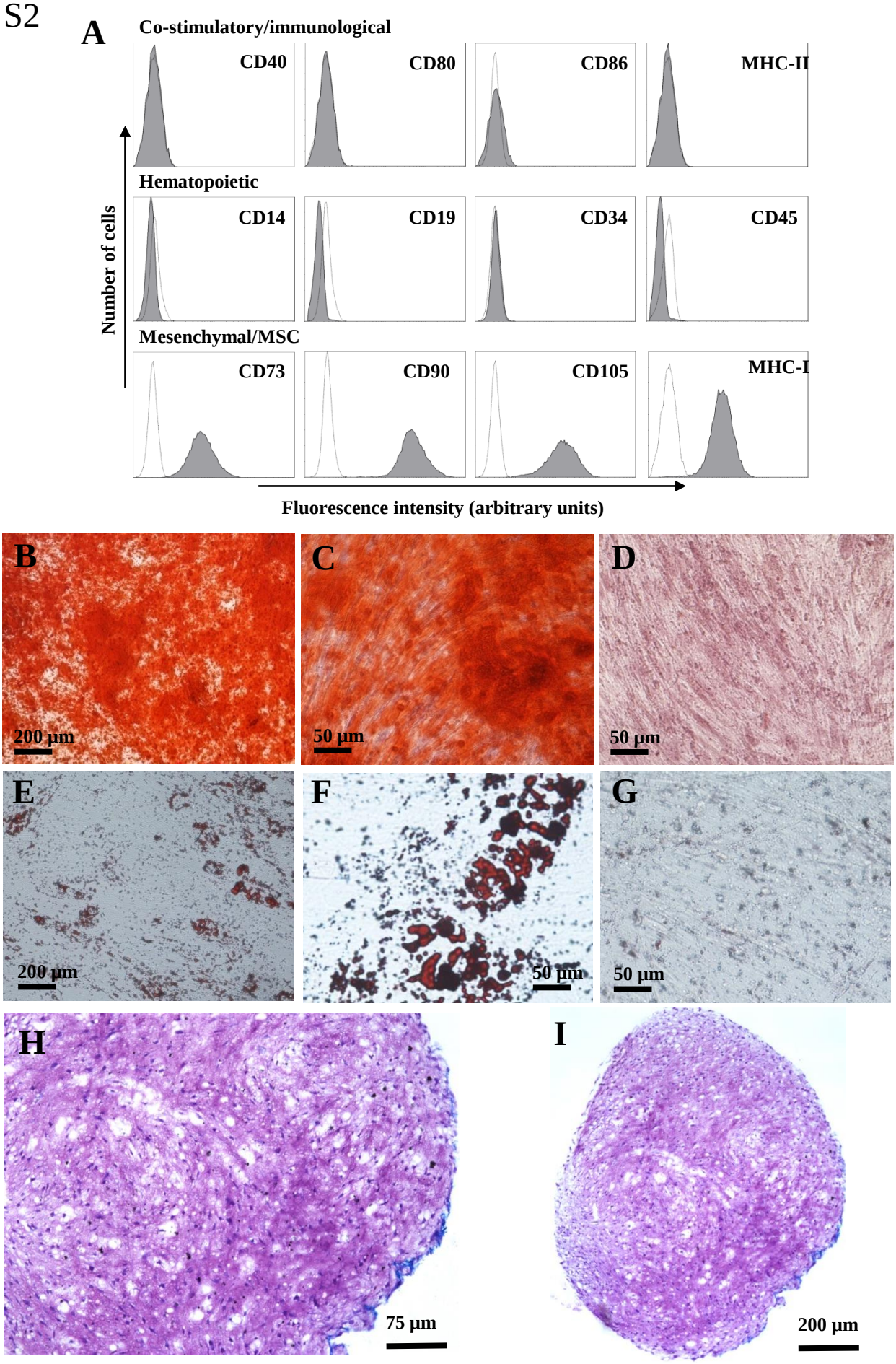
A
Co-stimulatory/immunological
CD40
CD80
CD86
MHC-II
Hematopoietic
CD14
CD19
CD34
CD45
Mesenchymal/MSC
CD73
CD90
CD105
MHC-I
Number of cells
Fluorescence intensity (arbitrary units)
B
200 µm
C
50 µm
D
50 µm
E
200 µm
F
50 µm
G
50 µm
H
75 µm
I
200 µm

Fig. S3

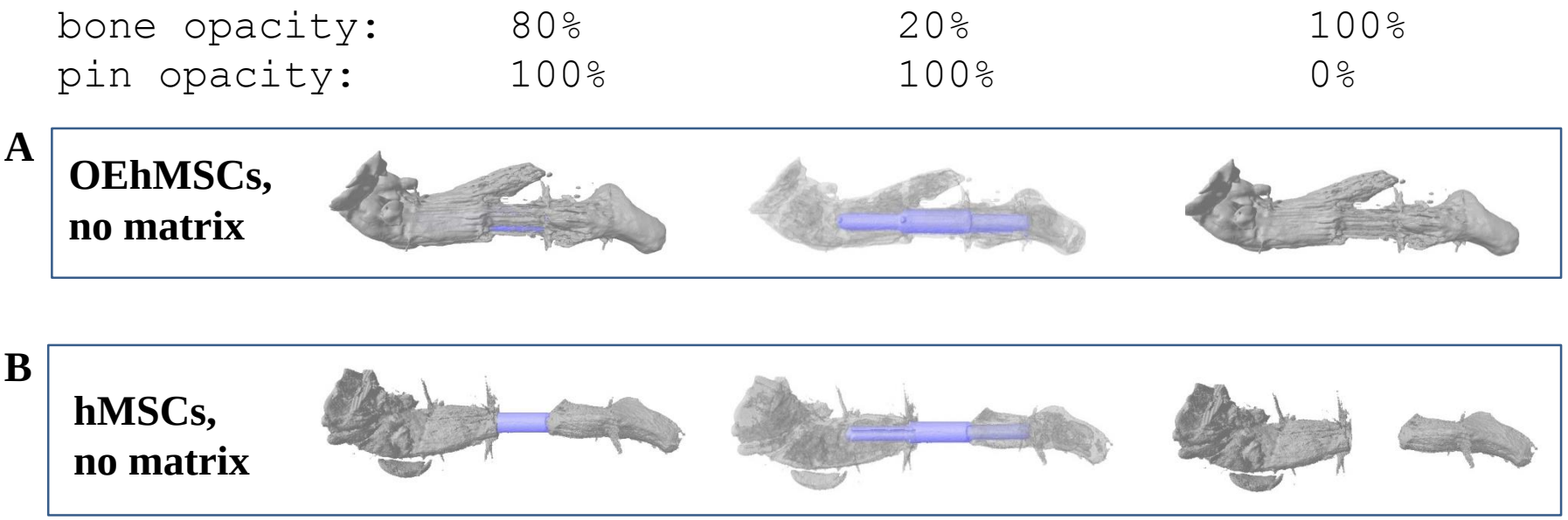
bone opacity: 80% 20% 100%
pin opacity: 100% 100% 0%
A
OEhMSCs,
no matrix
B
hMSCs,
no matrix

Fig. S4

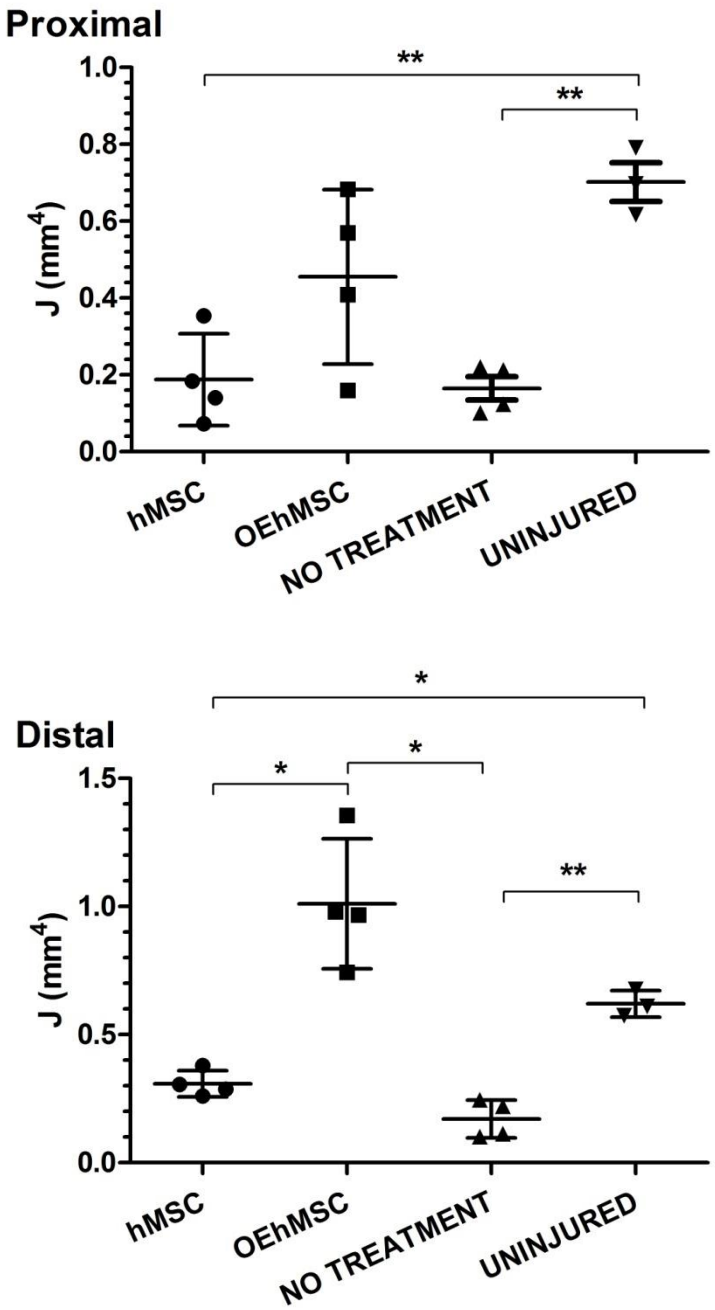
Proximal
**
**
1.0
0.8
0.6
0.4
0.2
0.0
J (mm4)
hMSC
OEhMSC
NO TREATMENT
UNINJURED
*
Distal
*
*
**
1.5
1.0
0.5
0.0
J (mm4)
hMSC
OEhMSC
NO TREATMENT
UNINJURED

Fig. S5

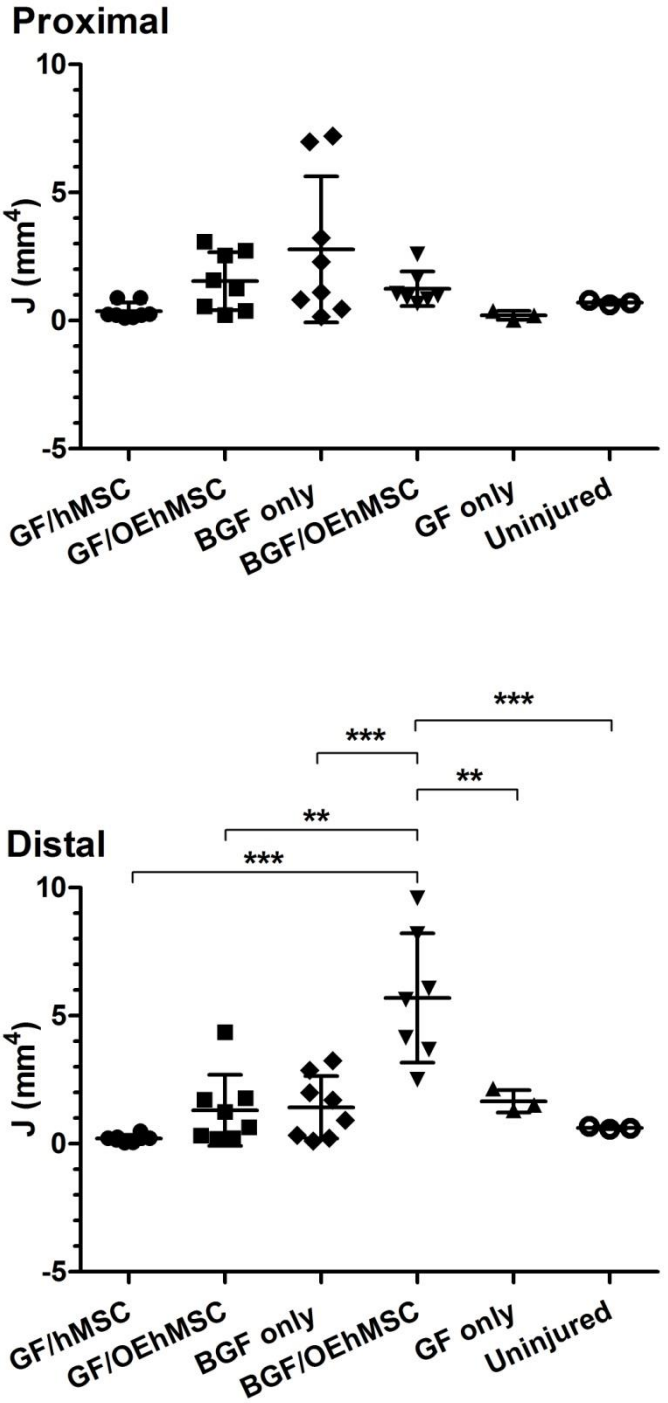
Proximal
10
5
0
-5
J (mm4)
GF/hMSC
GF/OEhMSC
BGF only
BGF/OEhMSC
GF only
Uninjured
***
***
**
**
***
Distal
10
5
0
-5
J (mm4)
GF/hMSC
GF/OEhMSC
BGF only
BGF/OEhMSC
GF only
Uninjured

Fig. S6

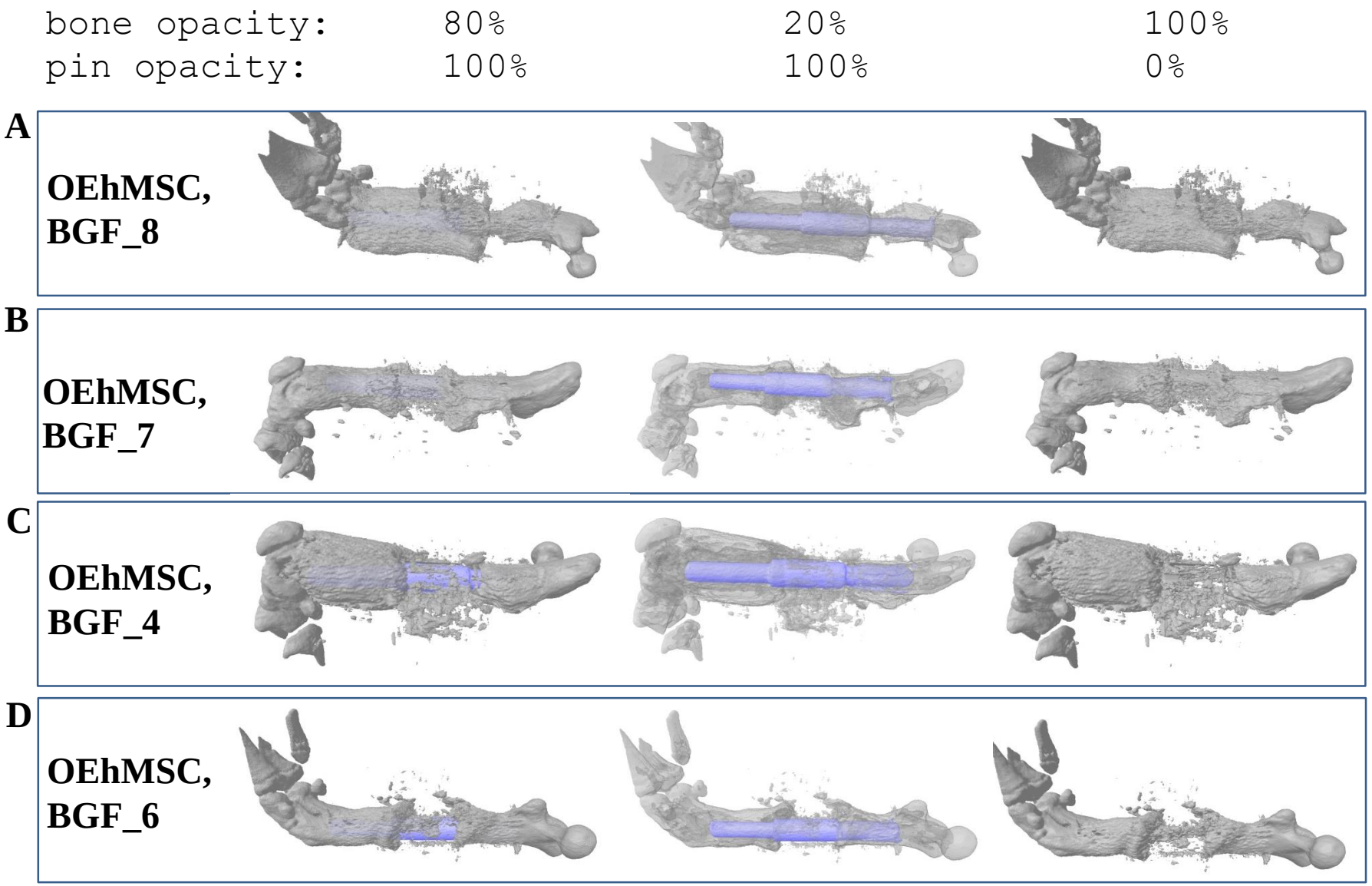
bone opacity: 80% 20% 100%
pin opacity: 100% 100% 0%
A
OEhMSC, BGF_8
B
OEhMSC, BGF_7
C
OEhMSC, BGF_4
D
OEhMSC, BGF_6

Fig. S7

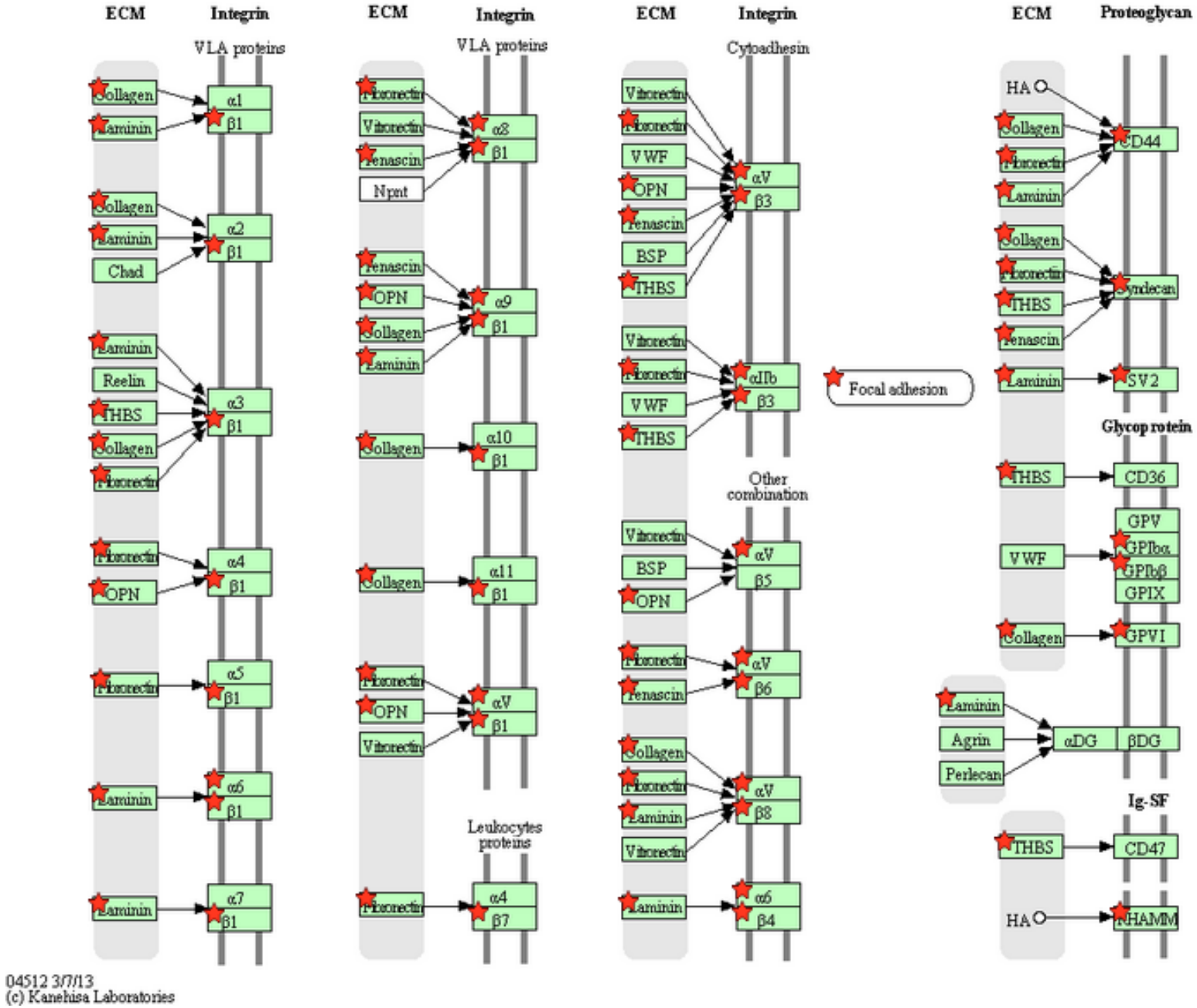

Fig. S8

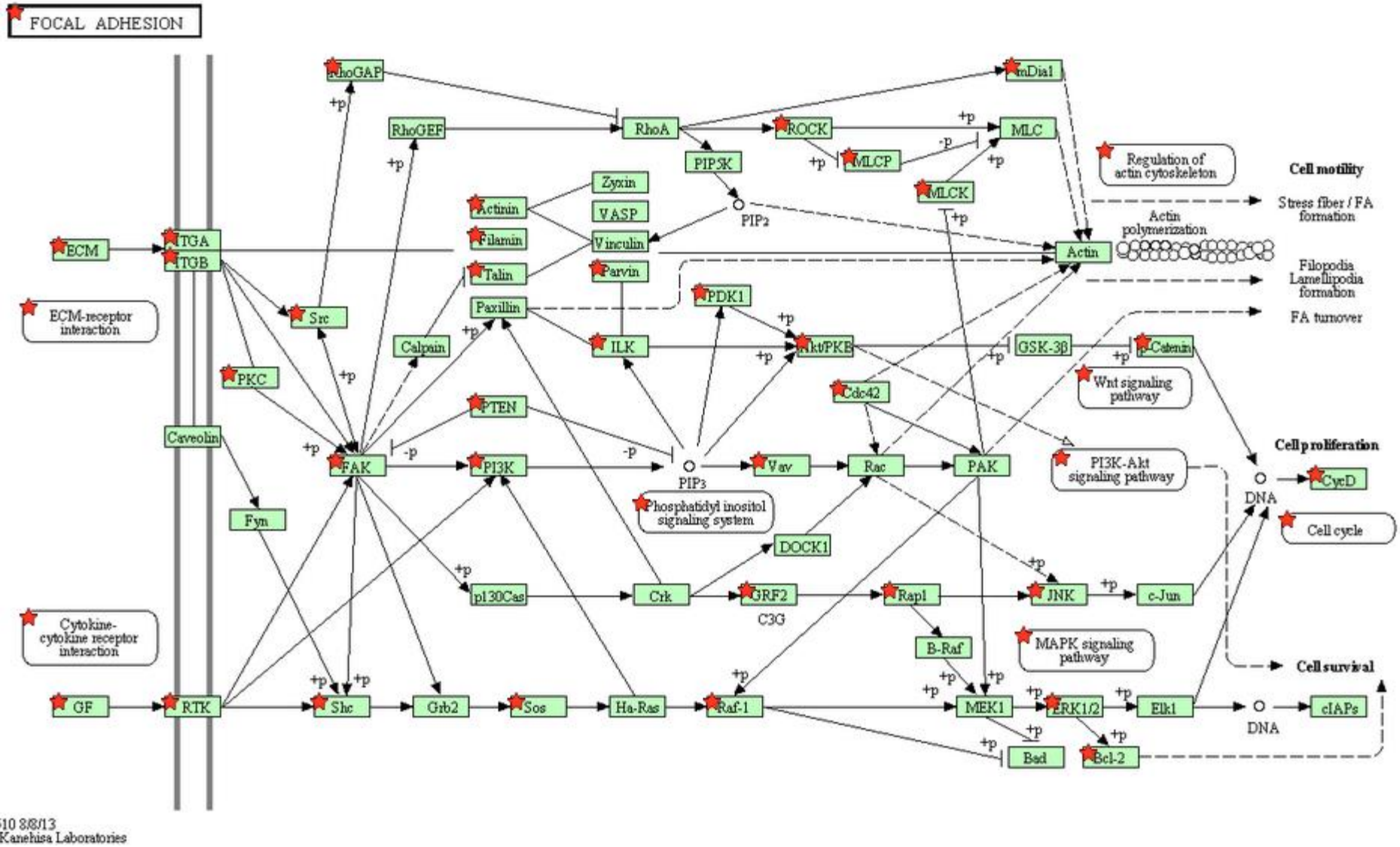
FOCAL ADHESION
ECM
ITGA
ITGB
ECM-receptor interaction
PKC
Caveolin
Fyn
Cytokine-cytokine receptor interaction
GF
RTK
RhoGAP
RhoGEF
Src
Calpain
Actinin
Filamin
Talin
Zyxin
VASP
Vinculin
Parvin
Paxillin
FAK
PTEN
PI3K
ILK
PDK1
Akt/PKB
PIP3
Phosphatidyl inositol signaling system
PIP2
PIP5K
RhoA
ROCK
MLCP
MLC
MLCK
mDia1
Regulation of actin cytoskeleton
Actin
Actin polymerization
Cell motility
Stress fiber / FA formation
Filopodia Lamellipodia formation
FA turnover
GSK-3β
β-Catenin
Wnt signaling pathway
Cdc42
Vav
Rac
PAK
PI3K-Akt signaling pathway
Cell proliferation
CycD
Cell cycle
DNA
DOCK1
p130Cas
Crk
GRF2
C3G
Rap1
JNK
c-Jun
B-Raf
MAPK signaling pathway
Cell survival
Shc
Grb2
Sos
Ha-Ras
Raf-1
MEK1
ERK1/2
Elk1
cIAPs
Bad
Bcl-2
04510 8/8/13
(c) Kanehisa Laboratories